Inorg. Chem. **2005**, *44*, 1125–1131

Disilver(I) Macrocycles: Variation of Cavity Size with Anion Binding

Nancy L. S. Yue, Michael C. Jennings, and Richard J. Puddephatt*

Department of Chemistry, University of Western Ontario, London, Canada N6A 5B7

Received October 15, 2004

Reaction of the N-methylated bis(amidopyridine) ligand, LL = C_6H_4(1,3-CONMe-4-$C_5H_4N)_2$, with the silver salts $AgNO_3$, AgO_2CCF_3, AgO_3SCF_3, $AgBF_4$, and $AgPF_6$ gave the corresponding cationic disilver(I) macrocycles [Ag_2-(μ-LL)$_2$]X_2, **2a**–**e**. The transannular silver···silver distance in the macrocycles varies greatly from 2.99 to 7.03 Å, and these differences arise through a combination of different modes of anion binding and from the presence or absence of silver···silver secondary bonding. In all complexes, the ligand adopts a conformation in which the methyl group and oxygen atom of the MeNCO units are mutually cis, but the overall macrocycle can exist in either boat (X = PF_6 only) or chair conformation. Short transannular silver···silver distances are found in complexes **2b**,**c**, in which the anions $CF_3CO_2^-$ and $CF_3SO_3^-$ bind above and below the macrocycle, but longer silver···silver distances are found for **2a**,**d**,**e**, in which the anions are present, at least in part, inside the disilver macrocycle. Easy anion exchange occurs in solution, and studies using ESI-MS indicate that the anion binding to form [Ag_2X-(μ-LL)$_2$]$^+$ follows the sequence X = $CF_3CO_2^-$ > NO_3^- > $CF_3SO_3^-$.

Introduction

There is much current interest in the synthesis and properties of self-assembled hybrid organic−inorganic macrocyclic or polymeric compounds, which form a class of molecular materials with potential applications as receptors.[1−10] Both the stereochemistry of the metal ion and the geometry of the ligand affect the final coordination topology, and it follows that metals such as silver(I), which can adopt several different coordination geometries, can yield a particularly rich array of supramolecular structures.[11,12]

Ligands containing one or more amide functionality have proved to be useful in self-assembly, since they give predictable patterns of hydrogen bonding that can add extra dimensionality and helicity to the supramolecular structures, in a biomimetic fashion. The analogous N-methylated amide functionality has not been exploited nearly as often, and potential applications are more limited since hydrogen bonding is not possible. Nevertheless, there is potential for new chemistry since the −N(Me)C(═O)− group tends to exist with the methyl and oxygen substituents mutually cis whereas the opposite conformation is most common for the −NHC(═O)− group[13−21] and this conformational difference affects the chemical and physical properties of the overall molecule.[22,23] For example, the amide group of the simple

* Author to whom correspondence should be addressed. E-mail: pudd@uwo.ca.

(1) Fujita, M.; Aoyagi, M.; Ibukuro, F.; Ogura, K.; Yamaguchi, K. *J. Am. Chem. Soc.* **1998**, *120*, 611−612.
(2) Fujita, M. *Chem. Soc. Rev.* **1998**, *27*, 417−425.
(3) Fujita, M.; Umemoto, K.; Yoshizawa, M.; Fujita, N.; Kusukawa, T.; Biradha, K. *Chem. Commun.* **2001**, 509−518.
(4) Sun Wei, Y.; Yoshizawa, M.; Kusukawa, T.; Fujita, M. *Curr. Opin. Chem. Biol.* **2002**, *6*, 757−764.
(5) Leininger, S.; Olenyuk, B.; Stang, P. J. *Chem. Rev.* **2000**, *100*, 853−907.
(6) Seidel, S. R.; Stang, P. J. *Acc. Chem. Res.* **2002**, *35*, 972−983.
(7) Stang, P. J.; Olenyuk, B. *Acc. Chem. Res.* **1997**, *30*, 502−518.
(8) Stang, P. J. *Chem.—Eur. J.* **1998**, *4*, 19−27.
(9) Jung, O.-S.; Kim, Y. J.; Lee, Y.-A.; Kang, S. W.; Choi, S. N. *Cryst. Growth Des.* **2004**, *4*, 23−24.
(10) Su, C.-Y.; Cai, Y.-P.; Chen, C.-L.; Smith, M. D.; Kaim, W.; Zur Loye, H.-C. *J. Am. Chem. Soc.* **2003**, *125*, 8595−8613.
(11) Khlobystov, A. N.; Blake, A. J.; Champness, N. R.; Lemenovskii, D. A.; Majouga, A. G.; Zyk, N. V.; Schroder, M. *Coord. Chem. Rev.* **2001**, *222*, 155−192.
(12) Zheng, S.-L.; Tong, M.-L.; Chen, X.-M. *Coord. Chem. Rev.* **2003**, *246*, 185−202.
(13) Itai, A.; Toriumi, Y.; Tomioka, N.; Kagechika, H.; Azumaya, I.; Shudo, K. *Tetrahedron Lett.* **1989**, *30*, 6177−6180.
(14) Yamaguchi, K.; Matsumura, G.; Kagechika, H.; Azumaya, I.; Ito, Y.; Itai, A.; Shudo, K. *J. Am. Chem. Soc.* **1991**, *113*, 5474−5475.
(15) Itai, A.; Toriumi, Y.; Saito, S.; Kagechika, H.; Shudo, K. *J. Am. Chem. Soc.* **1992**, *114*, 10649−10650.
(16) Azumaya, I.; Kagechika, H.; Yamaguchi, K.; Shudo, K. *Tetrahedron* **1995**, *51*, 5277−5290.
(17) Azumaya, I.; Yamaguchi, K.; Okamoto, I.; Kagechika, H.; Shudo, K. *J. Am. Chem. Soc.* **1995**, *117*, 9083−9084.
(18) Krebs, F. C.; Larsen, M.; Jørgensen, M.; Jensen, P. R.; Bielecki, M.; Schaumburg, K. *J. Org. Chem.* **1998**, *63*, 9872−9879.
(19) Azumaya, I.; Okamoto, I.; Nakayama, S.; Tanatani, A.; Yamaguchi, K.; Shudo, K.; Kagechika, H. *Tetrahedron* **1999**, *55*, 11237−11246.
(20) Jorgensen, M.; Krebs, F. C. *Tetrahedron Lett.* **2001**, *42*, 4717−4720.
(21) Lewis, F. D.; Long, T. M.; Stern, C. L.; Liu, W. *J. Phys. Chem. A* **2003**, *107*, 3254−3262.

10.1021/ic048549c CCC: $30.25
Published on Web 01/25/2005

Chart 1. Possible Conformations of Ligand **1**

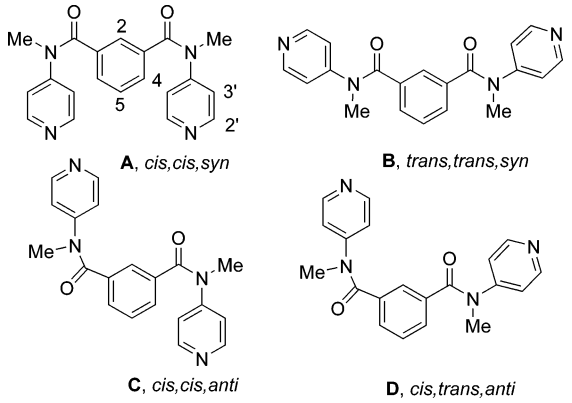

aromatic amide *N*-methylbenzanilide exists in the cis conformation in both the solution and the solid states, whereas the amide group of benzanilide exists in the trans conformation in the solid state. The cis conformation is common in *N*-alkyl amide derivatives,[12,13] including derivatives with two or more *N*-methyl amide groups, though there are exceptions to the rule.[11,13,14] The cis conformation at each of the *N*-methyl amide groups in the terpyridyl ligand 1,3,5-C_6H_3-{CON(Me)-3-C_5H_4N}$_3$ is preserved in its complexes with silver(I), copper(I), and copper(II), thus demonstrating that the preferred conformation can be used in designing new coordination compounds.[20]

This article reports the use of the N-methylated amidopyridine ligand LL = *N*,*N*′-dimethyl-*N*,*N*′-di-4-pyridylisophthalamide, **1** (Chart 1). The ligand could adopt several conformations, as illustrated in Chart 1, but it will be shown that it adopts distorted forms of the *cis*,*cis*,*syn* conformation **A** in all silver(I) complexes studied. The conformation is ideal for the formation of macrocyclic complexes of the type $[Ag_2(\mu\text{-LL})_2]^{2+}$. In such macrocycles the ring conformation can be the boat or the chair, and examples of both are known in related complexes.[24,25] For example, the conformation of the cationic macrocyclic complex $[Ag_2(\mu\text{-LL})_2]^{2+}$, with LL = 1,2-bis(benzimidazol-1-ylmethyl)benzene, is a chair or boat when the counterion is trifluoroacetate or triflate, respectively.[24] The aim of this work was to study the cationic complexes $[Ag_2(\mu\text{-LL})_2]^{2+}$ as receptors, having the potential ability to recognize different anions as a function of their size, shape, and coordinating ability.

Results and Discussion

Synthesis of Silver(I) Complexes. The disilver(I) macrocycles $[Ag_2(\mu\text{-LL})_2]X_2$, **2** [**2a**, X = NO_3; **2b**, X = CF_3CO_2; **2c**, X = CF_3SO_3; **2d**, X = BF_4; **2e**, X = PF_6], were simply prepared by reaction of equimolar amounts of the appropriate silver salt AgX with the ligand LL, as shown in Scheme 1.

(22) Kagechika, H.; Himi, T.; Kawachi, E.; Shudo, K. *J. Med. Chem.* **1989**, *32*, 2292−2296.
(23) Toriumi, Y.; Kasuya, A.; Itai, A. *J. Org. Chem.* **1990**, *55*, 259−263.
(24) Cai, Y.-P.; Su, C.-Y.; Zhang, H.-X.; Zhou, Z.-Y.; Zhu, L.-X.; Chan, A. S. C.; Liu, H.-Q.; Kang, B.-S. *Z. Anorg. Allg. Chem.* **2002**, *628*, 2321−2328.
(25) Tan, H.-Y.; Zhang, H.-X.; Ou, H.-D.; Kang, B.-S. *Inorg. Chim. Acta* **2004**, *357*, 869−874.

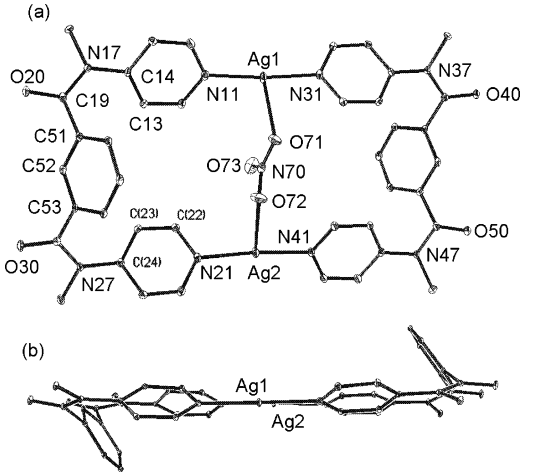

Figure 1. View of the structure of the nitrate complex **2a**: (a) top view; (b) side view with central nitrate group omitted. Selected bond parameters: Ag(1)−N(31) 2.156(3), Ag(1)−N(11) 2.167(3), Ag(1)−O(71) 2.528(2), Ag(2)−N(41) 2.155(3), Ag(2)−N(21) 2.158(3), Ag(2)−O(72) 2.559(3) Å; N(31)−Ag(1)−N(11) 174.6(1), N(31)−Ag(1)−O(71) 91.23(9), N(11)−Ag(1)−O(71) 92.93(9), N(41)−Ag(2)−N(21) 174.7(1), N(41)−Ag(2)−O(72) 97.8(1), N(21)−Ag(2)−O(72) 87.3(1)°.

Scheme 1

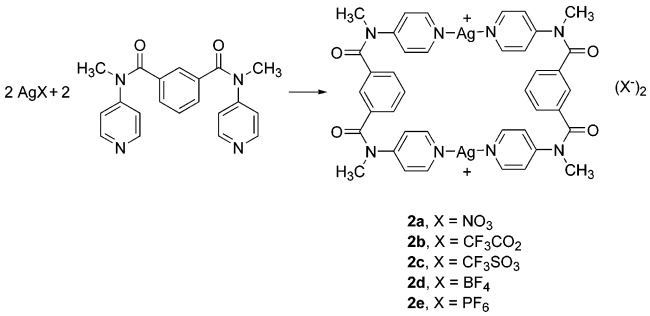

Table 1. Bond and Conformational Parameters (Å, deg) for the Macrocyclic Complexes **2**

complex	X	conf	AgAg	NAgN	θ^a	ϕ^b	ψ^c	α^d	β^e	γ^f
2a	NO_3	chair	6.38	175	56	3	25	7	42	52
2b	TFA	chair	2.99	159	102	0	63	32	43	125
2c	TRIF	chair	3.15	165	84	0	77	24	41	123
2d	BF_4	chair	7.03	178	54	0	26	18	40	41
2e[g]	PF_6	boat	6.47	172	45	90	32	21	37	36
2e[h]	PF_6	boat	6.80	175	45	90	30	20	37	37

[a] θ = mean interplanar angle aryl−Ag_2N_4. [b] ϕ = mean interplanar angle aryl−aryl. [c] ψ = mean interplanar angle py−Ag_2N_4. [d] α = mean torsion angle, CNCC. [e] β = mean torsion angle, py−CCNC. [f] γ = mean torsion angle, Ar−CCCO. [g] Solvate **2e**·$2CH_2Cl_2$·thf. [h] Solvate **2e**·$1.5CH_2Cl_2$·1.5EtOH.

The compounds were crystallized and their structures were determined in the solid state, to give information on the anion binding and its effect on the macrocyclic structures, as described below. The complexes are discussed in the order of the ligating ability of the anion, X^-, which is expected to follow the sequence X = NO_3, CF_3CO_2 > CF_3SO_3 > BF_4 > PF_6.

Disilver(I) Macrocycles in the Solid State. The structure of the nitrate complex **2a** is shown in Figure 1, with selected geometrical parameters listed in Table 1. It can be seen from Figure 1a that the complex is best considered as a cationic macrocycle $[Ag_2(\mu\text{-}NO_3)(\mu\text{-LL})_2]^+$, with one nitrate ion bound at the center of the macrocycle [Ag(1)O(71) =

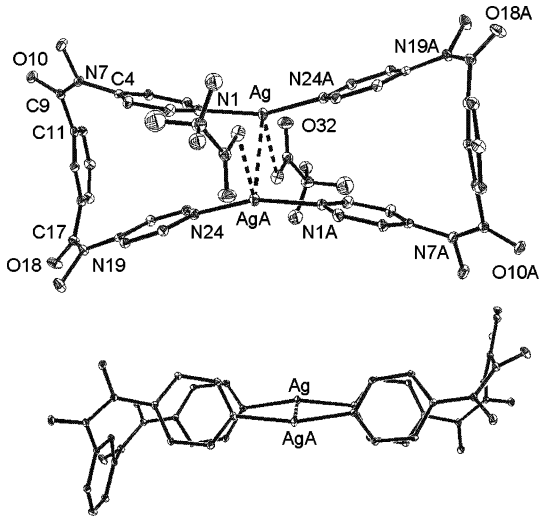

Figure 2. Top view (trifluoroacetate groups included) and side view (trifluoroacetate groups excluded) of the structure of complex **2b**. Selected bond parameters: Ag−N(24A) 2.167(5), Ag−N(1) 2.176(5), Ag···AgA 2.992(1) Å; N(24A)−Ag−N(1) 159.7(2), N(24A)−Ag−AgA 98.2(1), N(1)−Ag−AgA 92.3(1)°.

2.528(2), Ag(2)O(72) = 2.559(3) Å] while the other is present as the free anion and is not shown [closest contact Ag(2)O(81) = 3.19 Å]. The transannular silver−silver separation is 6.38 Å, which is obviously well suited to allow the macrocyclic host $[Ag_2(\mu\text{-LL})_2]^{2+}$ to accommodate the "guest" nitrate ion. The individual Ag···O bonds associated with nitrate ion binding are considered relatively weak, on the basis of the bond lengths and the fact that the angles N−Ag−N are not greatly distorted from linearity [N(31)−Ag(1)−N(11) 174.6(1), N(41)−Ag(2)−N(21) 174.7(1)°]. It will be convenient to discuss the conformation of the macrocycle in terms of the parameters given in Table 1 for the series of complexes. These parameters are based on the geometry of the aryl and pyridyl groups with respect to the Ag_2N_4 plane and on the dihedral angles associated with the amide groups. In the "ideal planar" conformation **A** (Chart 1), the aryl groups and the pyridyl groups would lie in the Ag_2N_4 plane. In complex **2a**, twisting at the amide group causes the aryl groups to lie above or below the plane (Figure 1b), and the extent of distortion can be measured by the mean angle θ [Table 1, **2a**, θ = 56°]. The two aryl groups are roughly parallel to each other (Figure 1b, angle ϕ between the two aryl groups = 3°), thus defining a chair conformation. Similarly, the pyridyl groups are twisted out of the plane by an average angle of ψ = 25° (Table 1). In complex **2a**, the central parts of the cis amide groups are close to planar [mean dihedral angle α = 7°, individual example C(14)N(17)C(19)C(51) = 8°]. However, considerable twisting out of the amide plane occurs for both the pyridyl groups [mean dihedral angle β = 42°, individual example C(13)C(14)N(17)C(19) = 41°] and aryl groups [mean dihedral angle γ = 52°, individual example C(52)C(51)C(19)O(20) = 51°].

The structure of the trifluoroacetate complex **2b** is shown in Figure 2, with selected geometrical parameters listed in Table 1. The most obvious difference compared to **2a** is the much shorter transannular distance [Ag···Ag = 2.992(1) Å in **2b**, 6.38 Å in **2a**], indicative of a secondary bonding

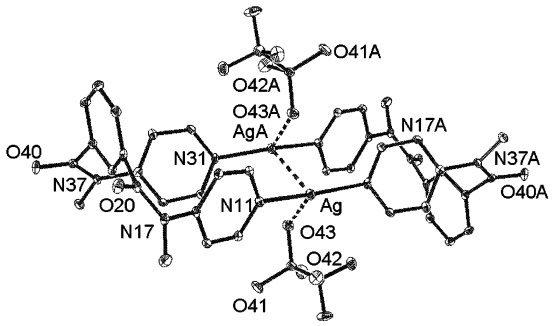

Figure 3. View of the structure of complex **2c**. Selected bond parameters: Ag−N(11) 2.150(5), Ag(A)−N(31) 2.153(4), Ag−Ag(A) 3.148(1) Å; N(11)−Ag−N(31A) 164.5(2)°.

interaction between the silver atoms. The angle N(24A)−Ag−N(1) = 159.7(2)° is considerably distorted from linearity in **2b**. Whereas a nitrate ion in **2a** was present inside the macrocycle, the trifluoroacetate ions in **2b** lie above and below the Ag_2N_4 plane and are more weakly bonded to silver. The shortest Ag···O contacts [Ag···O(31) = Ag(A)···O(31A) = 2.61 Å] are indicated by broken bonds in Figure 2. There are also relatively short contacts Ag···O(32) = Ag(A)···O(32A) = 2.90 Å and Ag···O(31A) = Ag(A)···O(31) = 2.93 Å so that the trifluoroacetate groups could be regarded as weakly bridging between the silver atoms. There is a center of symmetry at the midpoint between the two silver atoms so the conformations of the two ligands are identical. There are no great differences in bond angles within the amide groups of complexes **2a**,**b**, but there are major differences in the conformations. In particular the mean dihedral angle γ = 125° (Table 1) indicates inversion of the aryl group compared to complex **2a** (γ = 52°), while the angle between the aryl group and the Ag_2N_4 plane is obtuse in **2b** (θ = 102°) but acute in **2a** (θ = 56°) (Figure 2). The inversion center leads to a perfect chair conformation in **2b** (ϕ = 0°), and the pyridyl groups are closer to perpendicular to the Ag_2N_4 plane than in **2a** (ψ = 63° in **2b**, 25° in **2a**, Table 1). There is also much greater deformation of the amide group in **2b** than in **2a** (α = 7° in **2a**, 32° in **2b**).

The structure of the triflate complex **2c** is shown in Figure 3. A comparison of Figures 2 and 3 and the data listed in Table 1 illustrates that the structures of complexes **2b**,**c** are similar. For example, complex **2c** has a short contact Ag···Ag = 3.148(1) Å and a similar conformation at the amide group (Table 1). The macrocycle contains an inversion center and exists in the chair conformation. The triflate anions are located above and below the Ag_2N_4 plane, weakly bonded to silver. The shortest contacts Ag···O(43) = Ag(A)···O(43A) = 2.73 Å are illustrated with broken bonds in Figure 3, and there are also short contacts Ag···O(43A) = Ag(A)···O(43) = 2.82 Å, perhaps indicating weakly bridging triflate ions.

The structure of **2d** is shown in Figure 4. Comparisons of the geometrical data in Table 1 and the structures shown in Figures 1 and 4 illustrate a strong similarity between the structures of **2a**,**d**. In particular, complex **2d** exists as a macrocycle in the chair conformation (ϕ = 0°, Table 1), with a large transannular Ag···Ag separation of 7.03 Å and with

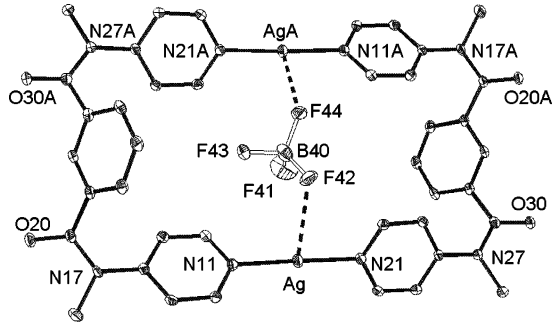

Figure 4. View of the structure of complex **2d**. Selected bond parameters: Ag−N(21) 2.125(4), Ag−N(11) 2.129(4) Å; N(21)−Ag−N(11) 177.7(1)°.

an anion that is at the center of the macrocycle and bridging between the two silver atoms (Figure 4). For complex **2d**, the cation $[Ag_2(\mu\text{-}BF_4)(\mu\text{-}LL)_2]^+$ contains a crystallographic inversion center and the bridging tetrafluoroborate anion is 50:50 disordered as a consequence, with only one component illustrated in Figure 4 for simplicity. As expected, the tetrafluoroborate bridges only weakly, with Ag(A)···F(44) = 2.73 Å and Ag···F(42) = 2.85 Å. The angle N(21)−Ag−N(11) = 177.7(1)° is very close to linear.

The structure of the hexafluorophosphate salt **2e** was determined as two different solvates, and the structures are shown in Figure 5. The structures are very similar, as shown by comparison of Figure 5a,b and by the average geometrical data given in Table 1. In both structures, the macrocycle exists in the boat conformation (ϕ = 90°, Figure 5c) in contrast to chair conformations adopted by complexes **2a**−**d** (ϕ = 0−3°). In the boat conformation, one side of the macrocycle is partly occupied by the mutually syn aryl groups and a loosely bound solvent molecule (tetrahydrofuran or dichloromethane in Figure 5a,b, respectively) is enclosed between the aryl groups, while the other side is open and is occupied by a bulky hexafluorophosphate anion in both solvates. The transannular distances Ag(1)···Ag(2) are similar at 6.47 Å in **2e**·$2CH_2Cl_2$·thf and 6.80 Å in **2e**·$1.5CH_2Cl_2$·1.5EtOH, and all angles N−Ag−N are close to linear. The shortest contacts between solvent molecules or $[PF_6]^-$ ions and silver(I) are shown as broken bonds in Figure 5, but all appear to represent weak interactions. The shortest contacts to solvent are Ag(2)···O(501) = 2.80 Å (Figure 5a) and Ag(1)···Cl(21) = 3.34 Å (Figure 5b), and the shortest contacts to $[PF_6]^-$ are Ag(2)···F(85) = 2.74 Å (Figure 5a) and Ag(2)···F(85) = 2.91 Å (Figure 5b).

Structures of the Complexes in Solution and Studies of Anion Binding. The ^{1}H NMR spectra of the complexes were consistent with the structures $[Ag_2(\mu\text{-}LL)_2]^{2+}$ but gave little information on anion binding or solvent association. Since the binding is expected to be weak in most cases, on the basis of the solid state structures, fast exchange is expected to occur in solution and so only "time averaged" NMR spectra are observed. The changes in the chemical shifts in the ^{1}H NMR spectra on ligand exchange were too small to allow the equilibrium constants to be determined. The result is that the equilibrium among $[Ag_2(\mu\text{-}LL)_2]^{2+}$, $[Ag_2(\mu\text{-}X)(\mu\text{-}LL)_2]^+$, $[Ag_2(\mu\text{-}X)_2(\mu\text{-}LL)_2]$, and solvated forms

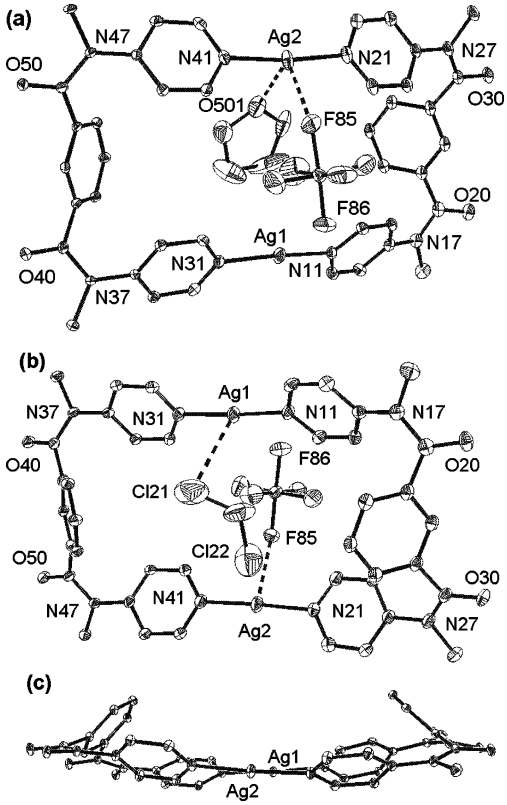

Figure 5. Views of the structure of **2e**: (a) as the solvate **2e**·$2CH_2Cl_2$·thf; (b) top view and (c) side view with PF_6^- anion and CH_2Cl_2 solvate omitted to show the boat conformation, as the solvate **2e**·$1.5CH_2Cl_2$·1.5EtOH. Selected bond parameters for **2e**·$2CH_2Cl_2$·thf: Ag(1)−N(11) 2.111(5), Ag(1)−N(31) 2.128(5), Ag(2)−N(21) 2.143(5), Ag(2)−N(41) 2.148(5) Å; N(11)−Ag(1)−N(31) 170.3(2), N(21)−Ag(2)−N(41) 173.0(2)°. Selected bond parameters for **2e**·$1.5CH_2Cl_2$·1.5EtOH: Ag(1)−N(11) 2.113(7), Ag(1)−N(31) 2.128(6), Ag(2)−N(21) 2.113(7), Ag(2)−N(41) 2.130(7) Å; N(11)−Ag(1)−N(31) 174.5(3), N(21)−Ag(2)−N(41) 176.1(3)°.

of these complexes cannot be elucidated by NMR. Hence the complexes were studied by ESI-MS as dilute solutions in methanol. All of the complexes **2** gave ESI-MS envelopes of peaks due to derivatives of the ligand **1** and its silver(I) complexes centered at m/z = 347, 453, and 799, corresponding to $[\mathbf{1} + H]^+$, $[\mathbf{1} + {}^{107}Ag]^+$, and $[\mathbf{1}_2 + {}^{107}Ag]^+$, respectively. The highest mass peaks for complexes **2a**−**e** were observed at m/z = 970, 1021, 1057, 995, and 1053, corresponding to $[Ag_2(\mathbf{1})_2X]^+$ with X = NO_3, CF_3CO_2, CF_3SO_3, BF_4, and PF_6, respectively. No significant ions containing the solvent molecules and no dicationic complexes such as $[Ag_2(\mathbf{1})_2]^{2+}$ were detected.

Anion exchange was then studied by ESI-MS. For standard solutions of complex **2b** in methanol solution, the peak height at m/z = 1021 due to $[Ag_2(\mathbf{1})_2(O_2CCF_3)]^+$ was found to be directly proportional to the concentration of **2b** (R^2 = 0.9952), thus allowing the concentration of $[Ag_2(\mathbf{1})_2(O_2CCF_3)]^+$ to be determined by ESI-MS. Addition of $Bu_4N^+CF_3SO_3^-$ or $Bu_4N^+NO_3^-$ led to a decrease in intensity of the peak at m/z = 1021 and a corresponding growth of a new peak at m/z = 1057 or m/z = 970 due to $[Ag_2(\mathbf{1})_2(O_3SCF_3)]^+$ or $[Ag_2(\mathbf{1})_2(NO_3)]^+$, respectively, as shown in Figure 6. Approximate equilibrium constants $K = [Ag_2(\mathbf{1})_2(X)]^+[CF_3CO_2^-]/[Ag_2(\mathbf{1})_2(O_2CCF_3)]^+[X^-]$ = 0.23 (X = CF_3SO_3) or

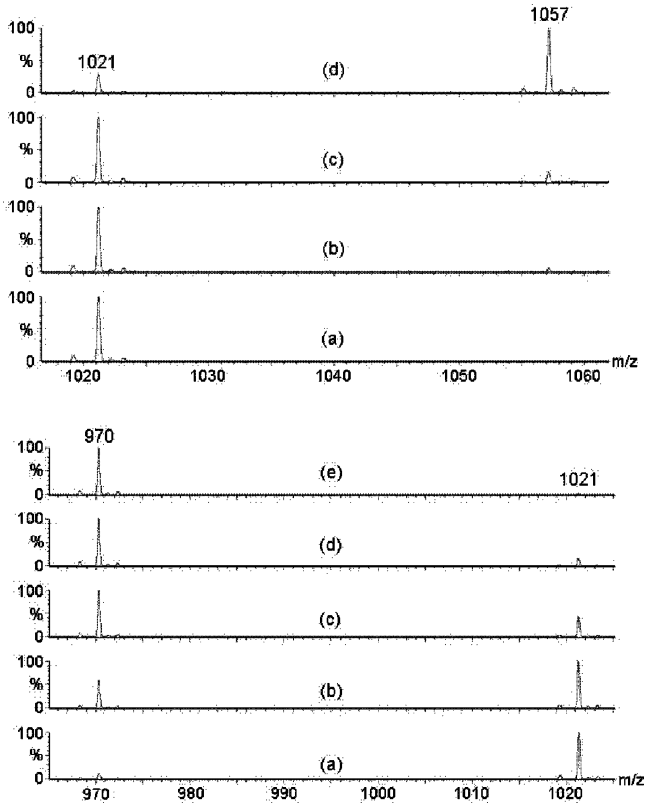

Figure 6. ESI-MS studies of anion exchange in the cationic disilver macrocycles $[Ag_2X(\mu\text{-LL})_2]^+$, by reaction of **2b** (X = CF_3CO_2) in methanol solution with $Bu_4N^+Y^-$. Top: Y = CF_3SO_3, with ratio **2b**:$Bu_4N^+Y^-$ (a) 1:0.8, (b) 1:1.2, (c) 1:2, and (d) 1:4. Bottom: Y = NO_3, with ratio **2b**: $Bu_4N^+Y^-$ (a) 1:0.8, (b) 1:1.2, (c) 1:1.6 (d) 1:2, and (e) 1:3.

0.37 (X = NO_3) were then determined, indicating the coordination sequence $X^- = CF_3CO_2^- > NO_3^- > CF_3SO_3^-$. This sequence is that expected from the pK_a values of the acids: CF_3CO_2H, 0.5 > HNO_3, −1.5 > CF_3SO_3H, −13.[23] If the structures in solution are similar to those in the solid state, the rather low discrimination between the anions X^- in $[Ag_2(\mathbf{1})_2(X)]^+$ indicates that there is little energy difference between the structure with the large cavity and the anion inside (X = NO_3) and the structure with the small cavity, with silver···silver bonding, and the anion outside (X = CF_3CO_2 or CF_3SO_3).

Conclusion

The cis conformation of the *N*-methyl amide group clearly favors the formation of the disilver(I) macrocycles $[Ag_2(\mu\text{-LL})_2]^{2+}$, rather than polymers, by self-assembly. In the solid state, complexes containing one or two loosely coordinated anions are observed (Figures 1−5), but in methanol solution, complexes with one associated anion are favored. In the solid state, the shortest Ag···O bonds to oxo anions are found in the nitrate complex **2a** [Ag···O = 2.53 Å], followed by the trifluoroacetate complex **2b** [Ag···O = 2.61 Å] and the triflate complex **2c** [Ag···O = 2.73 Å], consistent with a series reported previously for silver(I) complexes of thiobis(pyridine) and perhaps indicating that nitrate is the best ligand for silver(I).[24] However, the binding sequence in solution of trifluoroacetate > nitrate > triflate is that expected on the basis of the pK_a values of the corresponding acids and is perhaps more reliable.[23] Calculations by molecular mechanics indicate that the natural transannular distance in the macrocycles $[Ag_2(\mu\text{-LL})_2]^{2+}$ is in the range 6−7 Å, suggesting that the complexes **2a**,**d**,**e** are relatively strain-free. If the Ag··· Ag distance is constrained to be 3 Å, the additional ring strain is calculated to be in the region of 40 kJ mol^{-1}, and this is presumably compensated by the secondary silver···silver bonding in complexes **2b**,**c**. We are not aware of any precedents for the easy expansion and contraction of the cavity in disilver(I) macrocycles as a function of weak coordination by oxo anions.

Experimental Section

NMR spectra were recorded by using a Varian Mercury 400 spectrometer. Chemical shifts are quoted with respect to TMS, and the labeling scheme is given in Chart 1. We note difficulty in obtaining good H, N analytical data for some of the silver complexes reported below, but the C analyses are satisfactory and all complexes are characterized crystallographically.

***N,N′*-Dimethyl-*N,N′*-di-4-pyridylisophthalamide, 1,** was prepared by the literature procedure.[26] NMR in CD_2Cl_2: $\delta(^1H)$ = 8.41 [dd, 4H, J_{HH} = 3 Hz, 6 Hz, $H^{2'}$], 7.41 [m, 1H, H^2], 7.25 [m, 2H, H^4], 7.13 [m, 1H, H^5], 6.89 [dd, 4H, J_{HH} = 3 Hz, 6 Hz, $H^{3'}$], 3.41 [s, 6H, CH_3]; $\delta(^{13}C)$ = 170.2 [C═O], 152.5, 150.7, 136.1, 130.8, 129.2, 128.8, 121.2, 37.7 [Me]. Anal. Calcd for $C_{20}H_{18}N_4O_2$: C, 69.35; H, 5.42; N, 16.17. Found: C, 69.35; H, 5.68; N, 16.33.

Complexes $[Ag_2(\mu\text{-}\mathbf{1})_2]X_2$, 2. A typical procedure is described for **2b** (X = CF_3CO_2). To a clear solution of CF_3CO_2Ag (0.050 g; 0.226 mmol) in ethyl acetate (10 mL) was added a solution of ligand **1** (0.035 g, 0.156 mmol) in CH_2Cl_2 (10 mL). The solution was stirred overnight, and hexane (20 mL) was added to precipitate the product as a white solid, which was collected by filtration, washed with THF, and dried under vacuum. Yield: 0.12 g (45%). NMR in CD_2Cl_2/CD_3OD: $\delta(^1H)$ = 8.54 [d, 8H, J_{HH} = 7 Hz, $H^{2'}$], 7.77 [m, 4H, H^4], 7.60 [t, 2H, J_{HH} = 8 Hz, H^5], 7.05 [t, 2H, H^2], 6.82 [d, 8H, J_{HH} = 7 Hz, $H^{3'}$], 3.41 [s, 12H, CH_3]. Anal. Calcd for $C_{44}H_{36}Ag_2F_6N_8O_8$: C, 46.58; H, 3.20; N, 9.88. Found: C, 46.25; H, 3.75; N, 9.31. Colorless plate crystals of **2b**·$2CH_2Cl_2$ were grown by slow diffusion of hexane into a solution of **2b** in CH_2Cl_2/ethanol.

Similarly were prepared the following. **2a** (X = NO_3): yield 38%. The complex was insufficiently soluble to allow characterization by NMR. Anal. Calcd for $C_{40}H_{36}Ag_2N_{10}O_{10}$: C, 46.53; H, 3.51; N, 13.57. Found: C, 46.17; H, 3.42; N, 12.99. Colorless plate crystals of **2a**·$4H_2O$ were grown by slow diffusion of a solution of ligand **1** in CH_2Cl_2 into a solution of $AgNO_3$ in aqueous ethanol. **2c** (X = CF_3SO_3): yield 37%. NMR in CD_2Cl_2/CD_3OD: $\delta(^1H)$ = 8.54 [d, 8H, J_{HH} = 7 Hz, $H^{2'}$], 7.77 [m, 4H, H^4], 7.60 [t, 2H, H^5], 7.05 [t, 2H, H^2], 6.87 [d, 8H, J_{HH} = 7 Hz, $H^{3'}$], 3.43 [s, 12H, CH_3]. Anal. Calcd for $C_{42}H_{36}Ag_2F_6N_8O_{10}S_2$: C, 41.81; H, 3.01; N, 9.29. Found: C, 41.67; H, 3.12; N, 8.78. Colorless plate crystals of **2c**·$2CH_2Cl_2$ were grown by slow diffusion of hexane into a solution of **2c** in CH_2Cl_2/ethanol. **2d** (X = BF_4): yield 45%. NMR in CD_2Cl_2/CD_3OD: $\delta(^1H)$ = 8.47 [d, 8H, J_{HH} = 7 Hz, $H^{2'}$], 7.70 [m, 4H, H^4], 7.55 [t, 2H, H^5], 7.16 [m, 2H, H^2], 6.91 [d, 8H, J_{HH} = 7 Hz, $H^{3'}$], 3.45 [s, 12H, CH_3]. Anal. Calcd for $C_{40}H_{36}Ag_2B_2F_8N_8O_4$: C, 44.40; H, 3.35; N, 10.36. Found: C, 43.98; H, 2.41; N, 9.74. Colorless plate crystals of **2d**·$2.5CH_2Cl_2$ were grown by slow diffusion of a solution of ligand **1** in CH_2Cl_2/ethanol into a solution

(26) Qin, Z.; Jennings, M. C.; Puddephatt, R. J. *Inorg. Chem.* **2003**, *42*, 1956−1965.

Table 2. Crystallographic Data for Complexes **2**

	2a·4H_2O	**2b**·2CH_2Cl_2	**2c**·2CH_2Cl_2
formula	$C_{40}H_{44}Ag_2N_{10}O_{14}$	$C_{46}H_{40}Ag_2Cl_4F_6N_8O_8$	$C_{44}H_{40}Ag_2Cl_4F_6N_8O_{10}S_2$
fw	1104.59	1304.40	1376.50
T (°C)	−123(2)	−123(2)	−123(2)
λ (Å)	0.710 73	0.710 73	0.710 73
space group	$P2_1/c$ (No. 14)	$P2_1/c$ (No. 14)	$P\bar{1}$ (No. 2)
a (Å)	14.2860(2)	10.4961(2)	9.1836(4)
b (Å)	26.2471(4)	26.9664(5)	9.7625(5)
c (Å)	11.5842(2)	10.0162(1)	14.9279(9)
α (deg)	90	90	92.418(1)
β (deg)	103.271(1)	117.175(1)	105.768(2)
γ (deg)	90	90	90.421(2)
V (Å^3)	4227.68(11)	2522.06(7)	1286.60(12)
Z	4	2	1
D_{calcd} (g/cm^3)	1.735	1.718	1.777
μ (cm^{-1})	0.1008	0.1071	0.1136
R indices [$I > 2\sigma(I)$][a]			
R1	0.0368	0.0623	0.0538
wR2	0.0750	0.1711	0.1098
	2d·2.5CH_2Cl_2	**2e**·2CH_2Cl_2·THF	**2e**·1.5CH_2Cl_2·1.5EtOH
formula	$C_{42.50}H_{41}Ag_2B_2C_{l5}F_8N_8O_4$	$C_{46}H_{47}Ag_2Cl_4F_{12}N_8O_5P_2$	$C_{44.50}H_{48}Ag_2Cl_3F_{12}N_8O_{5.50}P_2$
fw	1294.44	1439.40	1394.94
T (°C)	−123(2)	−123(2)	−123(2)
λ (Å)	0.710 73	0.710 73	0.710 73
space group	$P2/c$ (No. 13)	$C2/c$ (No. 15)	$C2/c$ (No. 15)
a (Å)	16.9602(3)	28.1405(4)	28.4093(13)
b (Å)	9.5276(2)	21.1149(3)	20.7821(7)
c (Å)	17.7105(4)	19.6972(3)	19.9364(9)
α (deg)	90	90	90
β (deg)	113.429(1)	108.999(1)	109.061(2)
γ (deg)	90	90	90
V (Å^3)	2625.89(9)	11066.2(3)	11125.2(8)
Z	2	8	8
D_{calcd} (g/cm^3)	1.637	1.728	1.666
μ (cm^{-1})	0.1077	0.1052	0.0997
R indices [$I > 2\sigma(I)$[a]			
R1	0.0473	0.0695	0.0882
wR2	0.1271	0.1826	0.2384

[a] $R1 = \sum||F_o| - |F_c||/\sum|F_o|$; $wR2 = [\sum w(F_o^2 - F_c^2)^2/\sum w(F_o^2)^2]^{1/2}$.

of $AgBF_4$ in THF. **2e** (X = PF_6): yield 47%. NMR in acetone-d_6: $\delta(^1H)$ = 8.59 [m, 8H, $H^{2'}$], 7.69 [t, 2H, H^5], 7.43 [dd, 4H, H^4], 7.31 [m, 8H, $H^{3'}$], 7.27 [d, 2H, H^2], 3.52 [s, 12H, CH_3]. Anal. Calcd for $C_{40}H_{36}Ag_2F_{12}N_8O_4P_2$·$CH_2Cl_2$: C, 38.37; H, 2.98; N, 8.73. Found: C, 38.60; H, 3.07; N, 10.62. Colorless prism crystals of **2e**·2CH_2Cl_2·THF were grown by slow diffusion of a solution of ligand **1** in CH_2Cl_2/ethanol into a solution of $AgPF_6$ in THF, while similar crystals **2e**·1.5CH_2Cl_2·1.5EtOH were grown by slow diffusion of a solution of ligand **1** in CH_2Cl_2/ethanol into a solution of $AgPF_6$ in ethanol.

ESI-MS. All ESI mass spectra were recorded using a Micromass LCT spectrometer and were calibrated with NaI at concentration 2 μg/μL in 50:50 propan-2-ol/water. The injection flow rate was 10.0 μL/min in all experiments. A stock solution of **2b** in methanol (5×10^{-4} M) was used to prepare standard solutions of **2b** at various concentrations (2×10^{-4}, 3×10^{-4}, 4×10^{-4}, and 5×10^{-4} M). A linear relationship between the intensity at m/z = 1021 due to $[Ag_2(\mathbf{1})_2(O_2CCF_3)]^+$ vs [**2b**] was obtained with R^2 = 0.9952, showing that concentrations could be determined from the peak intensities under standard conditions.

The procedure for studying anion exchange between **2b** and $Bu_4N^+CF_3SO_3^-$ was as follows. A stock solution of $Bu_4N^+CF_3SO_3^-$ in methanol (5×10^{-3} M) was used to prepare standard solutions of $Bu_4N^+CF_3SO_3^-$ at varying concentrations. To a solution of **2b** in methanol (1 mL, 5×10^{-4} M) was added a solution of $Bu_4N^+CF_3SO_3^-$ in methanol (1 mL, 1×10^{-3} M). The reaction mixture was stirred under ambient conditions for 5 min, and ESI-MS was recorded to give the concentrations of $[Ag_2(\mathbf{1})_2(O_2CCF_3)]^+$ and $[Ag_2(\mathbf{1})_2(O_3SCF_3)]^+$. The equilibrium constant, $K = [[Ag_2(\mathbf{1})_2(O_3SCF_3)]^+][CF_3CO_2^-]/[[Ag_2(\mathbf{1})_2(O_2CCF_3)]^+][CF_3SO_3^-]$, was then estimated. The procedure was repeated at several concentrations of $Bu_4N^+CF_3SO_3^-$ to give the average equilibrium constant K = 0.23(1). The same procedure was used to study anion exchange between complex **2b** and $Bu_4N^+NO_3^-$ to give the average equilibrium constant $K = [[Ag_2(\mathbf{1})_2(NO_3)]^+][CF_3CO_2^-]/[[Ag_2(\mathbf{1})_2(O_2CCF_3)]^+][NO_3^-]$ = 0.37(6) (see Figure 6).

General Information on X-ray Data Collection and Reduction. Data were collected using a Nonius Kappa-CCD diffractometer using COLLECT (Nonius, 1998) software. The unit cell parameters were calculated and refined from the full data set. Crystal cell refinement and data reduction were carried out using the Nonius DENZO package. The data were scaled using SCALEPACK (Nonius, 1998). The SHELXTL-NT V6.1 (G. M. Sheldrick) program package was used to solve and refine the structure by direct methods, except for **2d**, which was solved by Patterson methods. Non-hydrogen atoms were refined with anisotropic thermal parameters, except where mentioned below. The hydrogen atom positions were calculated geometrically and were included as riding on their respective carbon atoms. X-ray data are collected in Table 2.

$[Ag_2(\mu\text{-}NO_3)(\mu\text{-}\mathbf{1})_2][NO_3]\cdot 4H_2O$, 2a. There were four water molecules, and all eight of their hydrogen atoms were found in the difference map. The O−H bonds were fixed at 0.84 Å and allowed to refine with thermal parameters tied to their respective oxygen atoms.

$[Ag_2(\mu\text{-}\mathbf{1})_2][CF_3CO_2]_2\cdot 2CH_2Cl_2$, 2b. There was an inversion center at the midpoint of the macrocycle. There was 50:50 disorder

of the fluorine atoms of the CF_3 group, and the F atoms were refined anisotropically with fixed C−F = 1.349 Å. The CH_2Cl_2 solvent molecule was refined with C−Cl distances fixed at 1.72 Å.

$[Ag_2(\mu\text{-}1)_2][CF_3SO_3]_2\cdot 2CH_2Cl_2$, **2c**. There was an inversion center at the midpoint of the macrocycle. The crystal was twinned around the 001 reciprocal axis, and the program WIN-GX was used to prepare the HKLF file for final refinement.

$[Ag_2(\mu\text{-}1)_2][BF_4]_2\cdot 2.5CH_2Cl_2$, **2d**. There was an inversion center at the midpoint of the macrocycle. The anions were refined at half-occupancy, with the components related by the inversion center; the B−F bonds were restrained to be identical, and the bond length was refined to a value of 1.363 Å. Two CH_2Cl_2 molecules were refined at $^1/_2$ occupancy with an anisotropic model, and one was refined at $^1/_4$ occupancy with an isotropic model. The C−Cl bond lengths were restrained to be 1.72 Å, and the chlorine atoms were restrained to be 2.86 Å apart.

$[Ag_2(\mu\text{-}1)_2][PF_6]_2\cdot 2CH_2Cl_2\cdot$THF, **2e***. The two anions were modeled as 1 full PF_6 and 2 half PF_6 anions. One $^1/_2$ PF_6 was on a symmetry element, and the other part shared the site with a CH_2Cl_2 molecule of solvation. The P−F bonds of the $^1/_2$ PF_6 were restrained to be identical (1.59 Å), and the F−F distances were restrained to be greater than 2.0 Å. The two CH_2Cl_2 molecules of solvation were located on four sites: three were modeled at $^1/_2$ occupancy complete with hydrogen atoms, and one, which was located on a symmetry element, was modeled without hydrogen atoms, with the C−Cl bond lengths restrained to be 1.72 Å. The presence of dichloromethane and tetrahydrofuran was confirmed by recording the ^{1}H NMR spectrum.

$[Ag_2(\mu\text{-}1)_2][PF_6]_2\cdot 1.5CH_2Cl_2\cdot 1.5$ethanol, **2e****. The structure was similar to **2e***, and treatment of PF_6 anions and CH_2Cl_2 molecules was as above. The $1^1/_2$ molecules of ethanol were modeled isotropically complete with hydrogen atoms. The presence of dichloromethane and ethanol was confirmed by recording the ^{1}H NMR spectrum.

Acknowledgment. We thank the NSERC (Canada) for financial support. R.J.P. thanks the Government of Canada for a Canada Research Chair.

Supporting Information Available: Tables of X-ray data in CIF format. This material is available free of charge via the Internet at http://pubs.acs.org.

IC048549C